LAWRENCE
LIVERMORE
NATIONAL
LABORATORY

LLNL-JRNL-407104

Ultrafast strain gauge: Observation of THz radiation coherently generated by acoustic waves

M. Armstrong, E. Reed, K.-Y. Kim, J. Glownia, W. M. Howard, E. Piner, J. Roberts

September 18, 2008

Nature Physics

Disclaimer

Ultrafast strain gauge: Observation of THz radiation coherently generated by acoustic waves

Michael R. Armstrong[a*], Evan J. Reed[a], Ki-Yong Kim[b], James H. Glownia[b], William M. Howard[a], Edwin L. Piner[c] and John C. Roberts[c]

[a]CMELS Directorate, Lawrence Livermore National Laboratory, Livermore, CA 94550

[b]CINT, Los Alamos National Laboratory, Los Alamos, NM 87545

[c]Nitronex Corp., 2305 Presidential Dr., Durham, NC 27703

Abstract

The study of nanoscale, terahertz frequency (THz) acoustic waves has great potential for elucidating material and chemical interactions as well as nanostructure characterization. Here we report the first observation of terahertz radiation coherently generated by an acoustic wave. Such emission is directly related to the time-dependence of the stress as the acoustic wave crosses an interface between materials of differing piezoelectric response. This phenomenon enables a new class of strain wave metrology that is fundamentally distinct from optical approaches, providing passive remote sensing of the dynamics of acoustic waves with ultrafast time resolution. The new mechanism presented here enables nanostructure measurements not possible using existing optical or x-ray approaches.

[*]Author to whom correspondence should be addressed at armstrong30@llnl.gov (Ph:925 423 5702)

Over the last decade, pioneering and innovative experiments using sub-picosecond lasers have demonstrated the generation and detection of acoustic and shock waves in materials with THz frequencies, the highest possible frequency acoustic waves.[1-5] In addition to groundbreaking demonstrations of acoustic solitons, these experiments have led to new techniques for probing properties of thin films and nanostructures.[6-8] THz frequency electromagnetic radiation has been used in applications as diverse as molecular and material excitations [9,10], charge transfer [11,12], imaging [13], and plasma dynamics [14]. However, existing approaches to detect and measure the time-dependence of THz frequency strain waves in materials currently employ direct optical probes – time resolved interferometry or reflectrometry.[2,15,16] Piezoelectric-based strain gauges have been employed in shock and strain wave experiments for decades, but the time resolution of such devices is limited to ~100 ps and slower, the timescale of electronic recording technology. We have recently predicted that THz frequency acoustic waves can be detected by observing THz radiation emitted when the acoustic wave propagates past an interface between materials of differing piezoelectric coefficients.[17,18] In this work, we present the first experimental observation of this fundamentally new phenomenon and demonstrate that it can be utilized to probe nanostructure properties inaccessible to existing optical and x-ray techniques.

As an acoustic wave traverses an interface between materials with differing piezo-electric response, polarization currents and concurrent radiation are predicted to be generated at the boundary. These currents radiate on the time scale of the strain changes.[17] For acoustic waves with characteristic frequencies of THz (corresponding to picosecond timescales), THz radiation is emitted. This phenomenon bears a close resemblance to the so-called transition radiation phenomenon that occurs when a charged particle propagates past an interface between two dielectric materials, generating

polarization currents and radiation from the interface. It is distinct from a narrowband, coherent THz emission mechanism that has been predicted to occur when a planar shock wave propagates through an ionic crystal.[19-21] When the interface is flat and some propagation properties of the strain wave are known, the time-dependence of the strain can be computed from the time-dependence of the radiated electric field. This enables the observation of ultrafast strain profiles in regions of a material not accessible to active probes such as those used in interferometry or reflectometry based methods.[2,22-24] This acoustic transition radiation (ATR) phenomenon has been predicted theoretically[17], but not yet observed experimentally. Some experimental evidence exists for other forms of electromagnetic radiation that may exhibit some correlation with acoustic processes.[23,25] Here we describe experimental results demonstrating acoustically generated THz radiation that is coherently related to the strain wave time-dependence via a well-understood physical mechanism. We emphasize that, in contrast to commonly employed THz generation[10,11,26,27], we report observations of radiation generated *by the THz frequency acoustic wave*, i.e. the signal is not conversion of an ultrashort optical pulse to THz radiation via the optical response of the sample.

The experimental scheme is shown in Fig. 1. In the present work, boundaries between regions of differing piezo-electric response are formed by a sub-micron thick layer of aluminum on gallium nitride, and a layer of AlN embedded in the GaN, as shown in the inset to Fig. 1. Piezoelectric wurtzite crystal structure GaN is oriented with its c-axis perpendicular to the sample surface. Terahertz radiation is generated when strain waves pass through the Al/GaN boundary and through the embedded AlN layer and the radiation is detected using conventional electro-optic sampling[26,27].

The acoustic wave is generated by focusing an ultrashort (~100 fs) optical pulse onto the Al layer, which heats the metal within ~3.5 ps[28] through a depth of about 50 nm.[28,29] Thermal expansion generates a wave with maximum strain on the order of -0.01 corresponding to pressures on the order of 1 GPa. Although the form of the acoustic wave is dependent primarily on material properties which have longer characteristic times than the pump pulse, the acoustic pulse generated at the Al surface is well synchronized with the pump.

Figure 2 shows the detected electric field for various thicknesses of Al coated on GaN. Around t=0 when the pump arrives at the Al surface, a fast THz signal is observed which is likely generated via the nonlinear optical response of the sample and/or photocurrent generation at the metal/air interface.[26] This signal is not believed to be related to acoustic emission but provides a convenient marker for t=0. At later times, the electric field exhibits slower variation corresponding to the acoustic pulse arrival at the Al/GaN. The arrival times at the interface vary linearly with the thickness of the Al layer in each sample (cf. Figure 2 inset), demonstrating a linear correlation between the time of emission and the acoustic transit time with a fitted acoustic velocity of 6.7 km/s +/- 6% (cf. 6.4 km/s sound speed in Al). Surface probe techniques[30] indicate that broadening of the pulse with increasing Al thickness primarily results from the distribution in sound speed as a function of grain orientation in the polycrystalline Al film. The ~1 mm pump diameter generates a strain wave that is significantly larger than the characteristic size of the crystallites in the Al film. We observe the duration of the fast rise in the acoustic profile to vary between 2 ps for thin Al layers (< 100 nm) to approximately 5 ps after propagation through 700 nm of Al. Data taken with a lower pump power (for a single Al thickness) exhibited electric field profiles with rise times equivalent to the higher power to within 1 ps. This suggests that polycrystalline acoustic speed

dispersion is a more significant effect than nonlinear effects at the strains generated in these experiments.

The term "nanoseismology"[23] has been proposed to characterize the study of thin film nanostructures using high frequency acoustic waves. Such studies to date have utilized optical techniques to observe reflected strain waves at surfaces. Acoustic transition radiation enables a new approach to materials characterization for piezoelectric structures. Structural details of a heterostructure may be determined by injecting a well-characterized acoustic profile and measuring the emitted electric field to determine the locations of boundaries between materials in the heterostructure. Figure 3 shows the electric field vs. time for three different samples with different Al layer thicknesses. A signal is generated when the wave cross the AlN layer because the piezoelectric coefficients for GaN and AlN differ. The transit time through the GaN layer is consistent at ~122 ps (GaN speed of sound: 8.00 +/- 0.02 km/s [5]). We attribute variations in the transit time to variation in the GaN thickness across the wafer. The transit delay between the Al/GaN signal and the AlN signal is consistent enough to establish that the observed peak results from the acoustic wave traversing the AlN layer. Since the single crystal GaN layer does not exhibit polycrystalline dispersion, scatter in the AlN signal likely indicates variation in the thickness of the 1 μm GaN layer which smears out the AlN peak. ATR may enable potentially nanometer scale resolution in a non-destructive measurement for comprehensive, rapid, on-line process control for thin film growth.

Figure 4 shows an expanded version of data from the sample coated with 260 nm of Al along with the stress estimated from the electric field distribution via an approach related to that of Reed *et*

al.[17] The recovered stress is qualitatively consistent with the expected form of an acoustic pulse excited by an ultrafast pump from a free surface.[3,8] For comparison, an ALE3D simulation of the stress assuming uniform illumination at 50 mJ/cm^2 fluence is also shown. Thermal expansion of the Al layer from pump illumination launches two counter-propagating compression pulses, the first towards the Al/GaN boundary and the second towards the Al free surface (at the Al/air boundary). The compression pulses have a time scale of roughly the spatial depth of the thermal deposition divided by the sound speed. The second compression pulse is reflected from the Al free surface with a 180 degree phase shift, resulting (with the first compression pulse) in a composite wave comprising an initial compression followed by a faster expansion to a tensile state (over the time scale of the thermal deposition) followed by a slower compression. The resulting acoustic profile is characteristic of an acoustic pulse generated by ultrafast laser excitation at a metal free surface.[4,8]

Figure 4 also shows the stress calculated from the first reflection from the Al/GaN boundary and the Al free surface, after the pulse has made two more passes through the Al layer. The reflected pulse exhibits a 180-degree total phase shift with each double pass, resulting from reflection from GaN (a higher impedance material than Al resulting in no sign change) and the free surface, which gives a 180-degree phase shift (a sign change). Although the fastest electric field rise times measured were 2-3 ps (implying < 0.5 THz emission), the stress recovery exhibits lower acoustic bandwidth. For instance, the fast, expansive portion of the stress in the 260 nm Al sample is about 5 ps (compared to a ~3 ps rise in the electric field), consistent with acoustic measurements in related systems using interferometry. [2,30] The simulated stress is similar qualitatively to the measured stress.

We expect some variation from the recovered stress due to polycrystalline dispersion in the experiment which is not present in the simulation[†].

Finally, the signal from the 10 nm layer of AlN is expected to take the form of a finite difference of the single interface signal over the acoustic transit time through the AlN layer (1 ps for a sound speed of 10 km/s in AlN). For comparison, a 1 ps finite difference of the single interface (Al/GaN) signal is shown in Fig. 4 superposed with the AlN signal. The finite difference and the AlN signal have the same qualitative form, but the AlN signal has a larger pulse width which we attribute to variation of the GaN thickness over the pump diameter.

We note that recovery of transient stress on nanometer length scales inside a sample is challenging using an active probe method such as interferometry, which requires a metallic interface to achieve nanometer spatial resolution, an otherwise optically transparent sample, and is adversely affected by acoustically modulated index variation in the sample, particularly for large amplitude acoustic waves.[31] In contrast, acoustically generated THz radiation may be detected independently from an arbitrary number of sufficiently well spaced interfaces along the acoustic wave trajectory. Also, owing to the longer wavelength of THz radiation, emission is less susceptible to optical inhomogeneity and pressure-induced index of refraction variation in the sample due to the wave. In particular, for the GaN heterostructure of Fig. 4, it would be extremely challenging to obtain the stress profile at the 10 nm AlN layer using an active optical probe or x-ray diffraction. We also note that the Al and Si surfaces of this sample prevent optical probes with photon energy above the Si bandgap from reaching the AlN layer.

[†] The simulation models a single crystal of Al.

In conclusion, we have observed THz radiation coherently emitted by an acoustic wave for the first time. This fundamentally new phenomenon has great potential for application as a remote, passive, and ultrafast strain gauge in semiconductor heterostructure metrology, acoustic and shock wave dynamics, and material investigations at extremely high strain rates and pressures.

Methods

The GaN sample is epitaxially grown on an atomically flat silicon (111) substrate by Nitronex, Inc., consisting of MOCVD grown layers[32] of (from free space to the Si substrate) 1 μm GaN, 10 nm of AlN, >400 nm of GaN, a proprietary transition layer, and the Si substrate. Each Al layer was sputter coated over a 4 mm diameter, with the thicknesses measured by Dektak, giving thicknesses of 700 +/- 40 nm, 560 +/- 30 nm, and 260 +/- 20 nm. The error in the thickness measurement was dominated by wafer warp. The Al surface is assumed to be flat with respect to the Al/GaN interface, with thickness variation of less than 10 nm, corresponding to less than 2 ps variation in acoustic transit time.

To obtain coupling between radiation modes and polarization currents that are along the c-axis (i.e. perpendicular to the sample surface), the sample is tilted 45 degrees off the optic axis. We directly detect the strain-induced electric field via electro-optic sampling with a 3 mm thick <110> ZnTe crystal in a pump-probe scheme with differential lock-in detection[10,26,27] using a low energy, ~100 fs duration, 800 nm probe pulse that is reflected from the back of the Si substrate, which has been polished to optical surface quality.

The 3 mm thick ZnTe crystal provides > 1 THz detection bandwidth[27], but does not exhibit strong THz reflections, simplifying the data analysis. Strong THz sample reflections are not evident in the

data (cf. Fig. 2, where ZnTe reflections would be observed at ~60 ps and sample reflections at 10 ps) with the maximum reflection amplitude observed < 20%. The ZnTe crystal is 2-3 mm from the sample along the probe beam. The field is sampled every 33 fs and the data is averaged over a moving window of 20 samples, reducing the time resolution to ~700 fs. The experiment is non-destructive (the pump fluence is below the damage threshold), and all experiments are multiple shot averages at half the pulse repetition rate of the laser, 500 Hz, with a 300 ms lock-in integration time. The pump pulse has 800 nm wavelength, ~100 fs duration, ~700 μJ energy, and 1.1 mm diameter (FWHM intensity).

We recover the time dependent stress from the electric field distribution using a method related to that described in Reed *et al.*[17] For the frequencies of interest, the electric field from the radiating source can be treated as a point time-dependent polarization with electric field at point $\dot{r}$ given by,

$$E(\dot{r},t) = -\hat{r}\times\hat{z}\times\hat{r}\frac{\ddot{P}(t-r/c)}{c^2 r} + \left[3\hat{r}(\hat{r}\cdot\hat{z}) - \hat{z}\right]\left(\frac{\dot{P}(t-r/c)}{cr^2} + \frac{p(t-r/c)}{r^3}\right) \qquad (1)$$

where $\dot{P}(t) = \sigma_{zz}(t) dA c_s$ is the current generated by the wave of area A and stress $\sigma_{zz}(t)$ in the GaN of piezoelectric coefficient d. In Equation (1), the polarization of the current is in the $\hat{z}$ direction and hats denote unit vectors. Equation (1) is solved for the time-dependence of the stress $\sigma_{zz}(t)$ given the electric field using a finite-difference scheme. We take $r = 6.5$ mm corresponding to the approximate optical path length between source and detector because the far-field term in Equation (1) dominates under the conditions of the experiments.[‡] While time-dependence of the stress is relatively straightforward, quantitative calculation of the stress magnitude is made challenging by the difficulties of calibrating the detection apparatus and complicated field and experiment geometry.

[‡] Equation (1) applies in a uniform medium and therefore represents an approximation to sample geometry utilized here.

Acknowledgements

We thank P. Celliers, R. Chau, R. Collins, J. Eggert, L. Fried, D. Hicks, N. Holmes, J. Nguyen, R. Patterson, and C. Tarver of LLNL, C. Bolme, D. Funk, D. Moore, and A. Taylor, of LANL, and R. Averitt of Boston University for helpful discussions. This work was supported by the LLNL LDRD program, the LANL CINT user program, and performed in part under the auspices of the U.S. Department of Energy by Lawrence Livermore National Laboratory under Contract DE-AC52-07NA27344.

Author contributions

MRA: experiments, data analysis; EJR: theory, simulations, data analysis; KYK: experiments, data analysis; JHG: facility, applications; WMH: simulations; ELP & JCR: sample fabrication

References

[1] Hao, H. Y. & Maris, H. J. Experiments with acoustic solitons in crystalline solids. *Phys. Rev. B* 64 (6), 064302 (2001).

[2] Gahagan, K. T. *et al.* Measurement of shock wave rise times in metal thin films. *Phys. Rev. Lett.* 85 (15), 3205-3208 (2000).

[3] Muskens, O. L. & Dijkhuis, J. I. High amplitude, ultrashort, longitudinal strain solitons in sapphire. *Phys. Rev. Lett.* 89 (28), 285504 (2002).

[4] Muskens, O. L., Akimov, A. V., & Dijkhuis, J. I. Coherent interactions of terahertz strain solitons and electronic two-level systems in photoexcited ruby. *Phys. Rev. Lett.* 92 (3), 035503 (2004).

[5] Wu, S. *et al.* Femtosecond optical generation and detection of coherent acoustic phonons in GaN single crystals. *Phys. Rev. B* 76 (8), 085210 (2007).

[6] Thomsen, C., Grahn, H. T., Maris, H. J., & Tauc, J. Surface Generation and Detection of Phonons by Picosecond Light-Pulses. *Phys. Rev. B* 34 (6), 4129-4138 (1986).

[7] Maris, H. J. Picosecond ultrasonics. *Sci. Am.* 278, 86 (1998).

[8] Saito, T., Matsuda, O., & Wright, O. B. Picosecond acoustic phonon pulse generation in nickel and chromium. *Phys. Rev. B* 67 (20), 205421 (2003).

[9] Grischkowsky, D., Keiding, S., Vanexter, M., & Fattinger, C. Far-Infrared Time-Domain Spectroscopy with Terahertz Beams of Dielectrics and Semiconductors. *J. Opt. Soc. Am. B-Opt. Phys.* 7 (10), 2006-2015 (1990).

[10] Ferguson, B. & Zhang, X. C. Materials for terahertz science and technology. *Nat. Mater.* 1 (1), 26-33 (2002).

[11] Beard, M. C., Turner, G. M., & Schmuttenmaer, C. A. Terahertz spectroscopy. *J. Phys. Chem. B* 106 (29), 7146-7159 (2002).

[12] Groot, M. L. *et al.* Coherent infrared emission from myoglobin crystals: An electric field measurement. *Proc. Natl. Acad. Sci. U. S. A.* 99 (3), 1323-1328 (2002).

[13] Chan, W. L., Deibel, J., & Mittleman, D. M. Imaging with terahertz radiation. *Rep. Prog. Phys.* 70 (8), 1325-1379 (2007).

[14] Kim, K. Y. *et al.* Measurements of Terahertz Electrical Conductivity of Intense Laser-Heated Dense Aluminum Plasmas. *Phys. Rev. Lett.* 100 (13), 135002 (2008).

[15] Evans, R. *et al.* Time- and space-resolved optical probing of femtosecond-laser-driven shock waves in aluminum. *Phys. Rev. Lett.* 77 (16), 3359-3362 (1996).

[16] Bolme, C. A., McGrane, S. D., Moore, D. S., & Funk, D. J. Single shot measurements of laser driven shock waves using ultrafast dynamic ellipsometry. *J. Appl. Phys.* 102, 033513 (2007).

[17] Reed, E. J., Armstrong, M. R., Kim, K. Y., & Glownia, J. H. Atomic-scale time and space resolution of THz frequency acoustic waves. *Phys. Rev. Lett.* 101 (1), 014302 (2008).

[18] Reed, E. J. *et al.* Terahertz radiation from shocked materials. *Mat. Today* 10 (7-8), 44-50 (2007).

[19] Reed, E. J., Soljacic, M., Gee, R., & Joannopoulos, J. D. Molecular dynamics simulations of coherent optical photon emission from shock waves in crystals. *Phys. Rev. B* 75 (17), 174302 (2007).

[20] Reed, E. J., Soljacic, M., Gee, R., & Joannopoulos, J. D. Coherent optical photons from shock waves in crystals. *Phys. Rev. Lett.* 96 (1), 013904 (2006).

[21] Reed, E. J., Soljacic, M., & Joannopoulos, J. D. Maxwell equation simulations of coherent optical photon emission from shock waves in crystals. *Phys. Rev. E* 75 (5), 056611 (2007).
[22] Geindre, J. P. *et al.* Frequency-Domain Interferometer for Measuring the Phase and Amplitude of a Femtosecond Pulse Probing a Laser-Produced Plasma. *Opt. Lett.* 19 (23), 1997-1999 (1994).
[23] Stanton, C. J. *et al.* Coherent phonons, nanoseismology and THz radiation in InGaN/GaN heterostructures. *Superlattices Microstruct.* 34 (3-6), 525-529 (2003).
[24] Sun, C. K., Liang, J. C., & Yu, X. Y. Coherent acoustic phonon oscillations in semiconductor multiple quantum wells with piezoelectric fields. *Phys. Rev. Lett.* 84 (1), 179-182 (2000).
[25] Hayes, B. Detonation electric effect. *J. Appl. Phys.* 38, 507 (1967).
[26] Mittleman, D. ed. Sensing with terahertz radiation. (Springer, New York, 2003).
[27] Gallot, G. & Grischkowsky, D. Electro-optic detection of terahertz radiation. *J. Opt. Soc. Am. B-Opt. Phys.* 16 (8), 1204-1212 (1999).
[28] Siwick, B. J., Dwyer, J. R., Jordan, R. E., & Miller, R. J. D. An atomic-level view of melting using femtosecond electron diffraction. *Science* 302 (5649), 1382-1385 (2003).
[29] Bonn, M. *et al.* Ultrafast electron dynamics at metal surfaces: Competition between electron-phonon coupling and hot-electron transport. *Phys. Rev. B* 61 (2), 1101-1105 (2000).
[30] Slayton, R. M. & Nelson, K. A. Picosecond acoustic transmission measurements. I. Transient grating generation and detection of acoustic responses in thin metal films. *J. Chem. Phys.* 120 (8), 3908-3918 (2004).
[31] Setchell, R. E. Refractive index of sapphire at 532 nm under shock compression and release. *J. Appl. Phys.* 91 (5), 2833-2841 (2002).
[32] Weeks, W. T., Piner, E. L., Gehrke, T., & Linthicum, K. J. U. S. Patent No. 6,617,060 (2003).

Figure legends

Figure 1: The experimental schematic. PBS is a polarizing beam separator, λ/2 and λ/4 are a half waveplate and quarter waveplate, respectively. The inset shows a cross section of the sample. The pump is incident on the Al coated side of the sample.

Figure 2: Electric field from Al/GaN interface vs. time. The plots are labeled by Al layer thickness. Dispersion in the shape of the pulse is primarily due to polycrystalline effects in the Al layer. An acoustic reflection in the Al layer radiates around 105 ps in the 260 nm Al coated sample. The transit times are labeled for the 260 nm trace. Inset: layer thickness vs. transit time in ps. A fit to the transit distance vs. time gives a sound speed of 6.7 km/s compared to the Al bulk sound speed 6.4 km/s.

Figure 3: Electric field vs. time for several Al thicknesses. The peak at ~70 ps in the 260 nm trace is an acoustic echo in Al. A time shift of the AlN signal in the 260 nm Al case suggests variations in the GaN layer thickness across the sample.

Figure 4: Electric field vs. time for the 260 nm Al sample (top black trace). After the stress wave initially encounters the Al/GaN interface, an acoustic echo is detected, corresponding to the acoustic wave traversing the Al layer two more times. The echo has the opposite sign compared to the initial Al/GaN signal. Signal from the AlN layer is detected at a time delay consistent with the thickness of the top GaN layer, 1 μm. The blue curve shows a time-shifted 1 ps finite difference of the Al/GaN signal overlaid on the AlN signal. The narrower width of the finite difference of the Al/GaN signal suggests roughness in the adjacent GaN layer. Also depicted is the stress calculated from the E-field (middle green trace) compared with the stress from a simulation of the acoustic profile (red, offset from the recovered stress) having the same qualitative form.

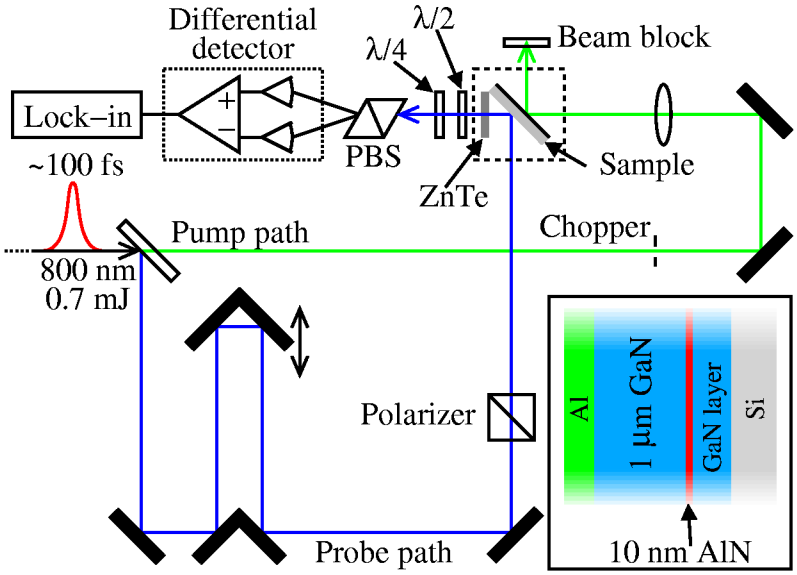

Figure 1: The experimental schematic. PBS is a polarizing beam separator, λ/2 and λ/4 are a half waveplate and quarter waveplate, respectively. The inset shows a cross section of the sample. The pump is incident on the Al coated side of the sample.

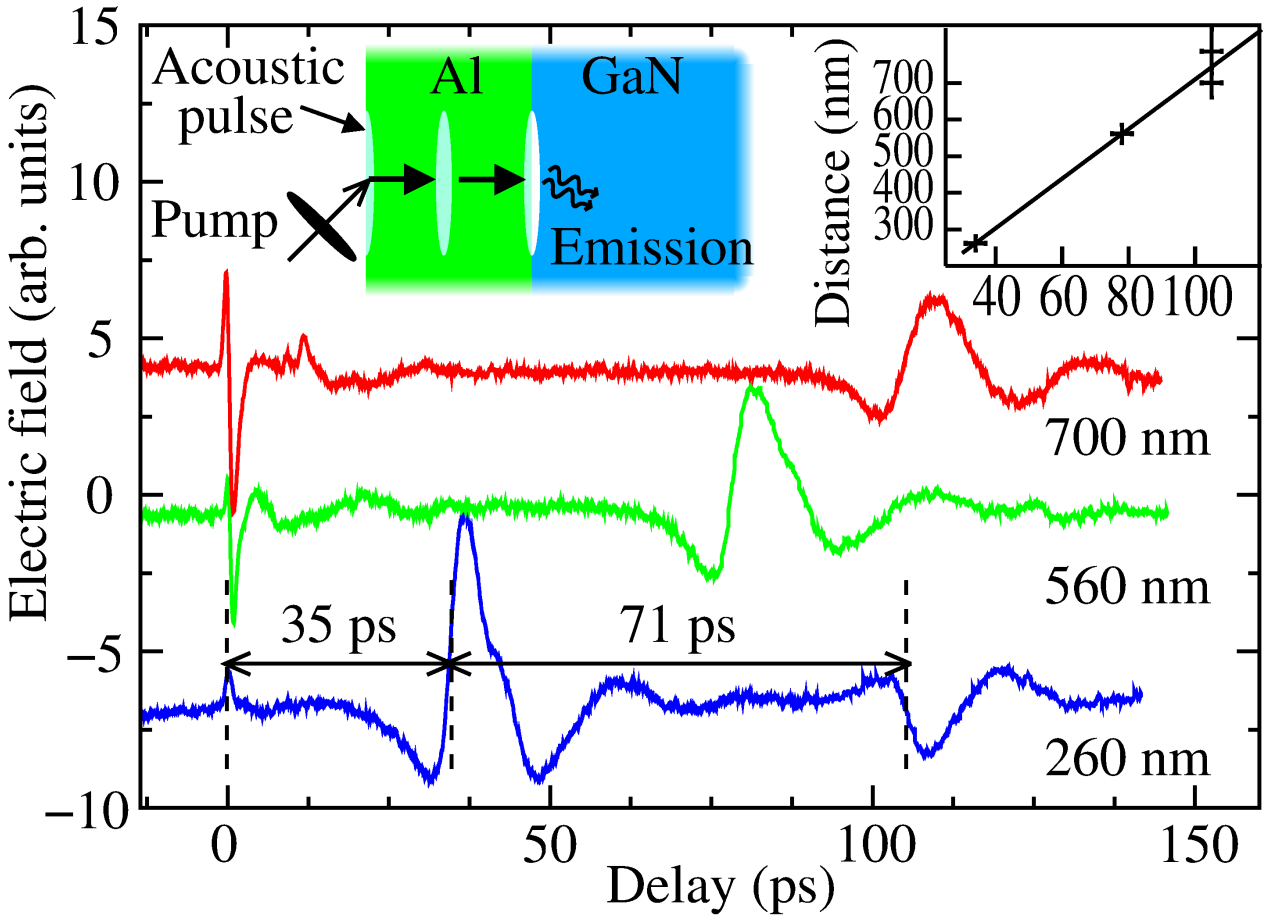

Figure 2: Electric field from Al/GaN interface vs. time. The plots are labeled by Al layer thickness. Dispersion in the shape of the pulse is primarily due to polycrystalline effects in the Al layer. An acoustic reflection in the Al layer radiates around 105 ps in the 260 nm Al coated sample. The transit times are labeled for the 260 nm trace. Inset: layer thickness vs. transit time in ps. A fit to the transit distance vs. time gives a sound speed of 6.7 km/s compared to the Al bulk sound speed 6.4 km/s.

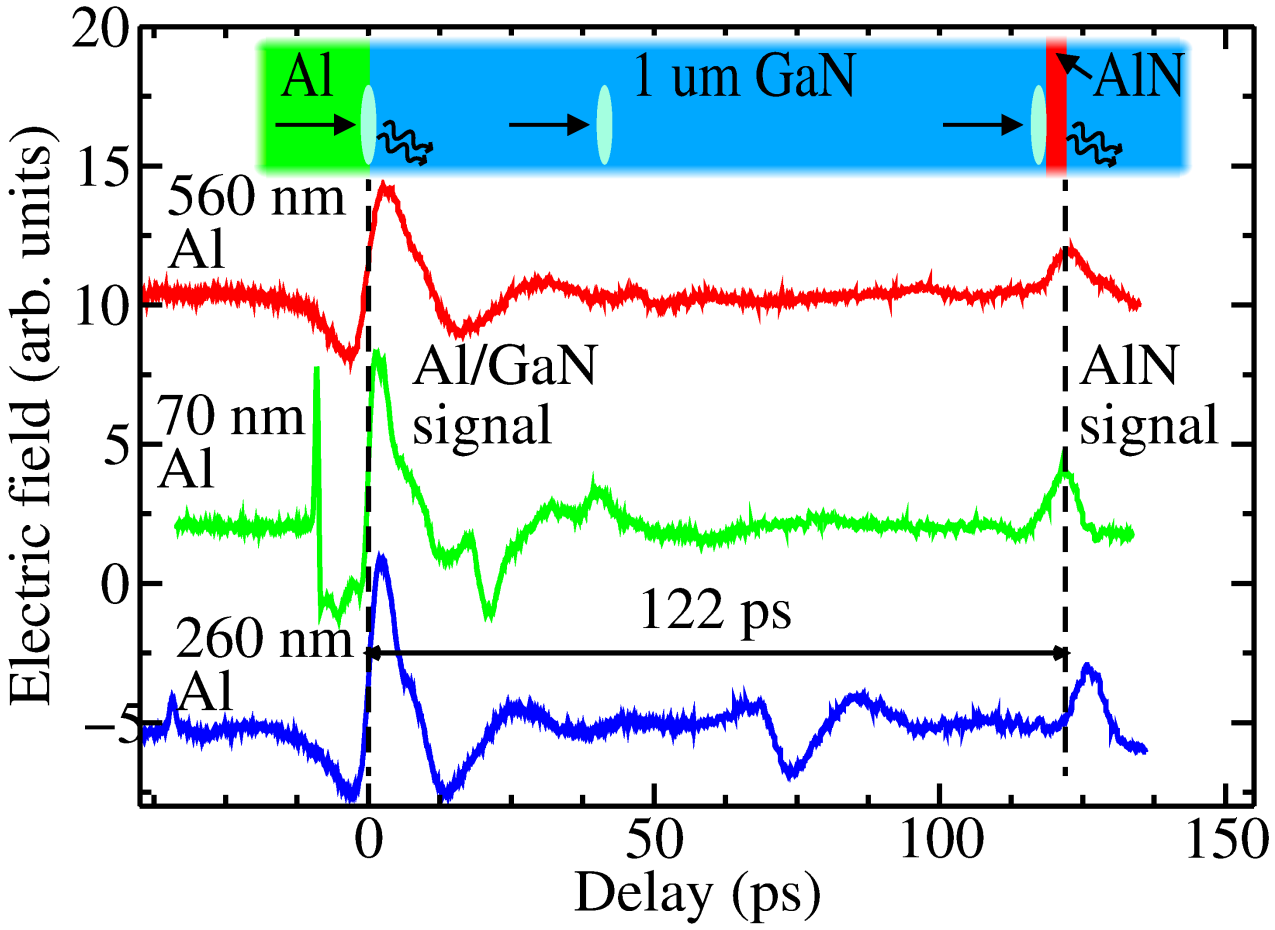

Figure 3: Electric field vs. time for several Al thicknesses. The peak at ~70 ps in the 260 nm trace is an acoustic echo in Al. A time shift of the AlN signal in the 260 nm Al case suggests variations in the GaN layer thickness across the sample.

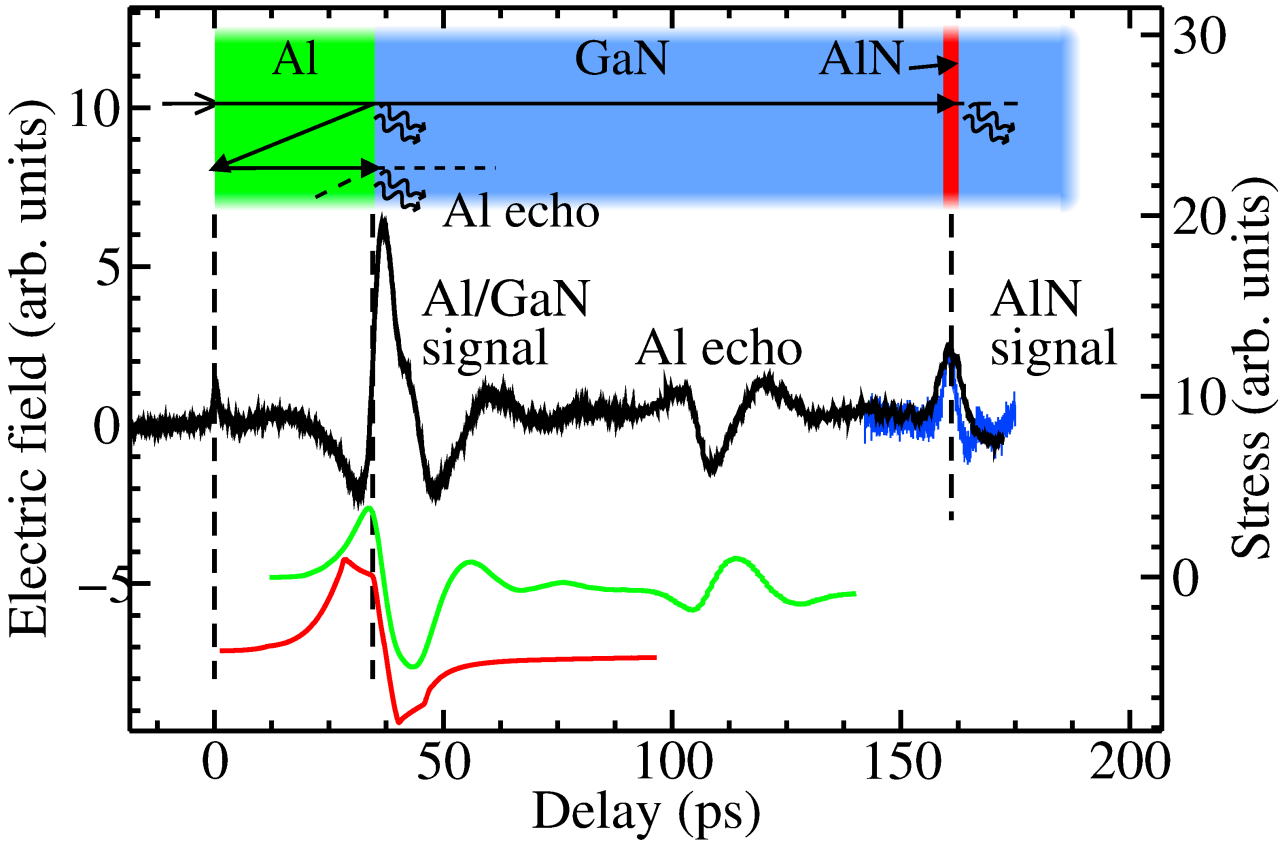

Figure 4: Electric field vs. time for the 260 nm Al sample (top black trace). After the stress wave initially encounters the Al/GaN interface, an acoustic echo is detected, corresponding to the acoustic wave traversing the Al layer two more times. The echo has the opposite sign compared to the initial Al/GaN signal. Signal from the AlN layer is detected at a time delay consistent with the thickness of the top GaN layer, 1 μm. The blue curve shows a time-shifted 1 ps finite difference of the Al/GaN signal overlaid on the AlN signal. The narrower width of the finite difference of the Al/GaN signal suggests roughness in the adjacent GaN layer. Also depicted is the stress calculated from the E-field (middle green trace) compared with the stress from a simulation of the acoustic profile (red, offset from the recovered stress) having the same qualitative form.